Investigation of reactive-ion-etch-induced damage of InP/InGaAs multiple quantum wells by photoluminescence

O. M. Steffensen and D. Birkedal
Mikroelektronik Centret, Building 345 East, Technical University of Denmark, DK-2800 Lyngby, Denmark

J. Hanberg and O. Albrektsen
Tele Danmark Research, Lyngsø Allé 2, DK-2970 Hørsholm, Denmark

S. W. Pang
University of Michigan, Department of Electrical Engineering and Computer Science, Ann Arbor, Michigan 48109-2122

The effects of CH_4/H_2 reactive ion etching (RIE) on the optical properties of an InP/InGaAs multiple-quantum-well structure have been investigated by low-temperature photoluminescence (PL). The structure consisted of eight InGaAs quantum wells, lattice matched to InP, with nominal thicknesses of 0.5, 1, 2, 3, 5, 10, 20, and 70 monolayers, respectively, on top of a 200-nm-thick layer of InGaAs for calibration. The design of this structure allowed etch-induced damage depth to be obtained from the PL spectra due to the different confinement energies of the quantum wells. The samples showed no significant decrease of luminescence intensity after RIE. However, the observed shift and broadening of the PL peaks from the quantum wells indicate that intermixing of well and barrier material increased with etch time. © *1995 American Institute of Physics.*

I. INTRODUCTION

Dry chemical etching techniques are important methods in the fabrication of optoelectronic components based on III-V compound semiconductors. In the fabrication of quantum wires, reactive ion etching (RIE) has been shown to be an effective technique[1,2] due to its highly anisotropic nature. However, the ion bombardment during the RIE process may introduce defects in the III-V heterostructures, which lead to degradation of the optical quality of the etched material. For RIE of InP/InGaAs heterostructures, the methane- or the ethane-based gas chemistry is found to be more effective than the chlorine-based gases.[3] Furthermore, in the etching of indium-containing compounds the methane gas mixture produces more straight sidewalls and smoother surfaces than the chlorine-based gases.

The optical characteristics of III-V heterostructures exposed to dry etching techniques and low-energy ions have previously been extensively studied.[4-7] Photoluminescence (PL) has been shown to be an excellent nondestructive tool in characterizing the induced damage in the buried layers. In this article we present the results of a PL study on a carefully designed structure containing InP/InGaAs quantum wells. The wells were grown with decreasing widths resulting in a correlation between depth and spectral position of the PL peaks. Thus, the penetration depth of the process-induced damage can be obtained from the PL spectra of the epitaxial structure.

In Sec. II we describe the experimental conditions of the present work. These include the growth of the heterostructure, the RIE conditions, and the PL setup. In Sec. III we present and discuss the results. In Sec. III A the PL results from the as-grown samples are presented. The experimental spectra are compared with the results of an envelope function calculation of the confinement energies of the quantum wells. The PL results from the dry-etched samples are presented and discussed in Sec. III B. Finally, we summarize in Sec. IV.

II. EXPERIMENT

The investigated InP/InGaAs multiple-quantum-well structure was grown by low-pressure organometallic vapor-phase epitaxy on a semi-insulating Fe-doped InP [100] substrate using trimethylindium, trimethylgallium, arsine, and phosphine as sources. The InGaAs and the InP layers were deposited with growth rates of 0.69 and 1.46 Å/s, respectively, as deduced from growth of thick layers. The structure consists of eight $In_{0.57}Ga_{0.43}As$ quantum wells and a thick layer of $In_{0.57}Ga_{0.43}As$ above the buffer layer for calibration. Estimated from the growth times, the InGaAs well layers have nominal thicknesses of 0.5, 1, 2, 3, 5, 10, 20, and 70 monolayers (ML). The well layers are hereafter denoted no. 1, no. 2, no. 3, no. 4, no. 5, no. 6, no. 7, and no. 8, respectively. The calibration layer of InGaAs has a thickness of 200 nm, sufficient to be free of the quantum confinement. Between each InGaAs layer, an InP spacer with a nominal thickness of 18 nm was grown. The entire quantum-well structure is grown on a 396 nm InP buffer layer. Finally, a 30 nm InP capping layer for protection of the wells was grown. Hence, the total thickness of the grown layers is approximately 800 nm.

Nine different samples from the wafer described above have been etched in CH_4/H_2 by RIE. During the etch the pressure in the etch chamber was 15 mTorr and the bottom electrode was kept at a temperature of 35 °C. In order to ensure the onset of the plasma, each process was started with a 2 s etch at 30 mTorr. The CH_4 and H_2 flows were 15 and 50 sccm, respectively. The etch chamber was cleaned in an oxygen plasma between each etch. The rf power was varied from 50 to 248 W, and the etch time was varied from 30 to 500 s. For each setting of the rf power, three samples were etched
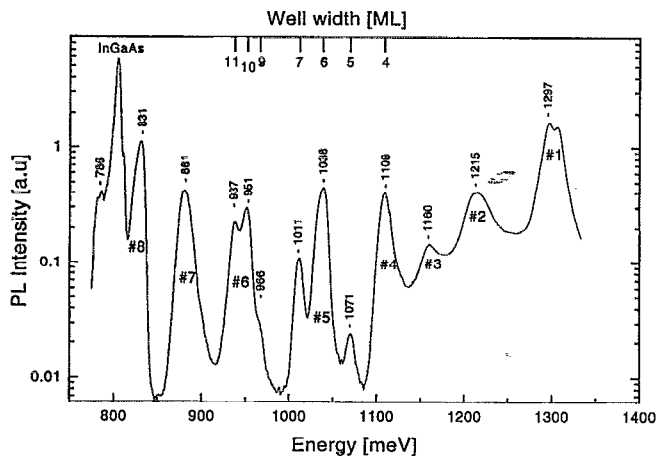
FIG. 1. PL spectrum from the as-grown InP/InGaAs multiple-quantum-well structure obtained at 4 K with a laser output power of 0.2 mW. Note that a logarithmic intensity scale has been used. The peaks are labeled by numbers indicating the eight quantum wells. The well width of some of the peaks has been deduced from an envelope function calculation. These are indicated in monolayers (ML) on the top axis.

with different etch times. A step in the samples was made by covering half of the sample by a thick piece of InP during the etch, so that we were able to measure the etch depths with a profilometer. This approach also allowed a comparison of the PL of an etched area and an unprocessed surface.

The PL spectra were obtained at 4 K using a continuous-flow cryostat with liquid helium as coolant. The 488 nm line of an argon-ion laser was used for excitation. The PL spectra were recorded with an excitation power of 0.2 mW. The laser light was focused onto the samples with a spot diameter of approximately 0.5 mm. The luminescence was dispersed through a 0.67 m spectrometer (McPherson) with a 600 groves/mm grating and detected by a liquid-nitrogen-cooled Ge p-i-n detector (North Coast EO 817L). Standard lock-in technique was used for data acquisition.

III. RESULTS AND DISCUSSION

A. PL from as-grown samples

Figure 1 shows a PL spectrum from an as-grown sample of the wafer described above. Note that a logarithmic intensity scale is used in Fig. 1 to enhance the display of the low-intensity peaks. A high-intensity peak at 0.804 eV and eight smaller peaks at 0.831, 0.881, 0.951, 1.038, 1.109, 1.160, 1.215, and 1.297 eV, respectively, are observed. There are high- and low-energy shoulders of the 0.951 eV peak and a high-energy shoulder of the 1.297 eV peak. Furthermore, small peaks are present at 1.011 and 1.071 eV. Finally, a low-intensity shoulder is noticed at 0.786 eV. PL spectra from other samples of the wafer showed the same qualitative behavior in their PL spectra as the spectrum shown in Fig. 1; however, the spectral position of the individual peaks varied systematically up to 15 meV across the wafer due to a variation in alloy composition.

We assign the peak at 0.804 eV in Fig. 1 to the electron-hole (eh) transition in the thick layer of InGaAs. The peak

positions of this peak varied between 0.803 and 0.817 eV across the wafer. These observations indicate that the composition variation of the InGaAs layer is significant. The broad low-energy shoulder observed at 0.786 eV is presumably due to a Zn- or Fe-related impurity transition in the thick layer of InGaAs as observed by Juang et al.[8] The eight smaller peaks, indicated in Fig. 1, are assigned to exciton transitions in the eight InGaAs quantum wells. The peaks show an increasing energy shift with decreasing well width due to the quantum size effect.

The observed transition energies of the eight wells have been compared with an envelope function calculation of the confinement energies.[9] At 4 K band gaps of 0.811 and 1.4236 eV for InGaAs and InP, respectively, have been used for the calculations. An effective electron mass of $0.041m_0$ and a heavy-hole mass of $0.465m_0$ have been used for InGaAs and an electron mass of $0.0765m_0$ and a heavy-hole mass of $0.485m_0$ have been used for InP.[10] Finally, a conduction-band discontinuity ΔE_c of 42% (Ref. 11) has been applied. We have assumed an exciton binding-energy dependence on the well width as measured by Lin et al.[12]

There is a qualitative agreement between the measured and calculated well transition energies as seen in the inset of Fig. 2, where the observed energy shift due to confinement is plotted against the nominal well width. We observe increasing energy shift with decreasing well width due to the quantum size effect. However, for the smaller well widths, we observe a significant discrepancy between the measurements and the calculations. The measured energies are in general 50–200 meV below the calculated energies for small well widths. The discrepancy increases with decreasing well width. This is a well-known phenomenon for InP/InGaAs quantum wells with well widths thinner than 5 nm, and it is believed to be due to the formation of $InAs_{1-x}P_x$ islands at the interfaces around the wells.[13,14]

Figure 2 shows the calculated (open circles) and the measured (solid squares) energy splittings, i.e., the energy difference between PL peaks from two well regions differing by 1 ML in width: $\Delta E = E_{n-1}^{PL} - E_n^{PL}$, where n is the number of monolayers. The labels and arrows in the figure indicate from which PL peaks the splittings are measured. By comparing the measured and the calculated energy shifts we conclude that the two shoulders of the 0.951 eV PL peak are due to 9 and 11 ML islands in the 10 ML well. Similar island formation is also observed for well no. 5. The deviations between the measured and calculated PL peaks for the 4–1 ML well widths do not allow definite identification of PL peaks from well no. 3 to no. 1. In general, we observe that the actual well widths are larger than the well widths deduced from growth rate data obtained for thick layers.

B. PL from reactive-ion-etched samples

For each rf power setting of 50, 149, and 248 W three samples have been etched. The process data for the samples are listed in Table I. The average etch depths measured by a profilometer are listed in Table I. In general the etch depths varied roughly 10 nm across the samples. The measured etch depths as a function of etch time are plotted in Fig. 3.

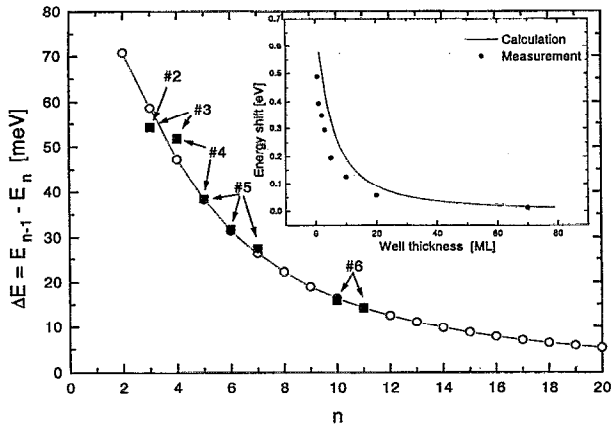J. Appl. Phys., Vol. 78, No. 3, 1 August 1995

Steffensen et al.   1529

FIG. 2. Measured energy splittings (solid squares) of the PL peaks from the as-grown MQW structure compared to an envelope function calculation (open circles and line). Labels and arrows indicate the well numbers from whose PL peaks the splitting have been measured. The inset shows the measured energy shifts as a function of nominal well width compared to the calculation.

Figure 4 shows the PL spectra from etched samples exposed to a rf power of 50 W. The PL spectrum labeled "no-etch" was taken from the part of the sample which had been covered during the etch and, hence, had not been etched. The spectral positions of the PL peaks from the quantum wells have been indicated by numbers and arrows in the figure. The three lower spectra were obtained from etched parts of the samples.

In the PL spectrum labeled "120 s-etch," the peak from the well no. 1 has decreased substantially in intensity as compared with the PL spectrum of the unetched region. The PL intensity from well no. 2 has also decreased in intensity. The results from the depth measurements indicate that well no. 1 is removed from most of the sample; however, from the etch depth variations across the sample it is expected that the well is still present in some regions. Indeed, this is reflected in the spectrum by the decrease of the PL signal from the well. The decrease in the PL signal from well no. 2 is caused by the partial removal and possible damage of this well during the etch. The remaining part of the spectrum seems to be unaffected by the etch.

TABLE I. List of etched samples with etching conditions and the measured etch depth.

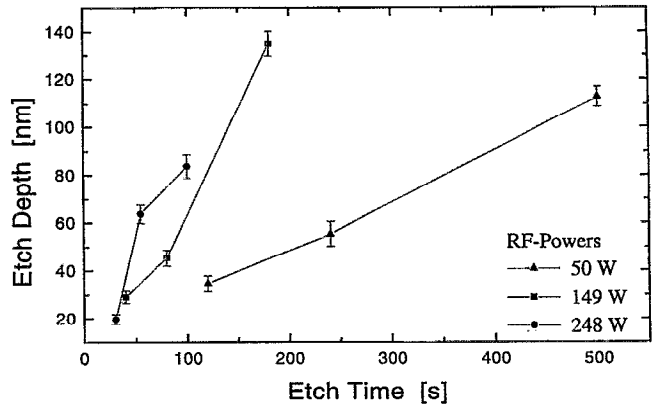| rf power (W)	Etch time (s)	Bias (V)	Etch depth (nm)
50	120	−238	34.6±3.2
50	240	−241	55.4±5.1
50	500	−240	112.7±4.1
149	40	−424	29.1±2.7
149	80	−422	45.3±3.4
149	180	−428	134.9±5.3
248	30	−540	19.7±1.1
248	55	−543	63.7±3.8
248	100	−543	83.6±4.9

FIG. 3. The measured etch depths of the CH_4/H_2 RIE of the InP/InGaAs MQW structure. The labels refer to the applied rf powers.

In the spectrum for the 240 s etch, we observe that the PL peak from well no. 1 has disappeared. The intensities of the peaks from wells no. 2, no. 3, and no. 4 have also decreased. It is also noticed that there is a shift of the peaks from wells no. 5, no. 6, and no. 7 toward higher energy. For the 500 s etch, the PL peaks from the five thinnest wells have disappeared. Again an energy shift of the peaks from wells no. 5, no. 6, and no. 7 is observed. Whereas the peak from well no. 6 has become broader, the peaks from well no. 8 and the calibration layer have become more narrow.
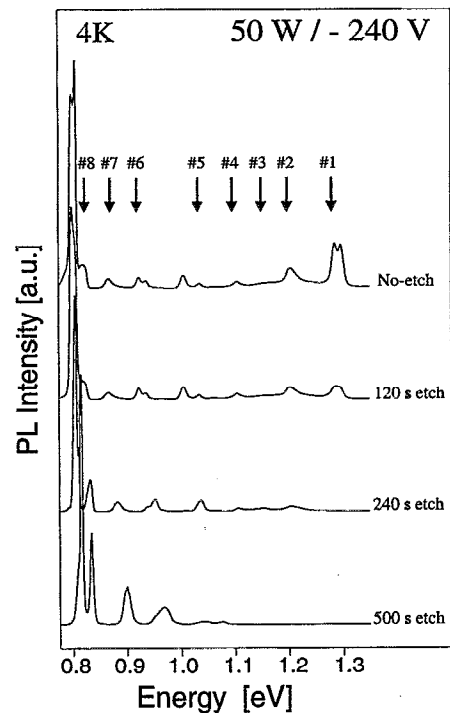

FIG. 4. PL spectra at 4 K after RIE with a rf power of 50 W. The numbers at the upper spectrum indicate the approximate PL peak positions of the individual quantum wells.

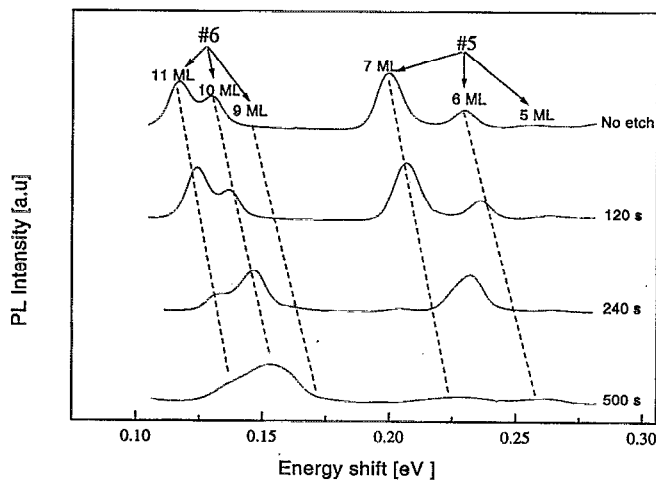1530   J. Appl. Phys., Vol. 78, No. 3, 1 August 1995

Steffensen et al.

FIG. 5. An expanded view of the peaks from wells no. 5 and no. 6 as shown in Fig. 4. The abscissa is the energy relative to the PL peak of the InGaAs calibration layer. The dotted lines illustrate the energy shift of the peaks.

The shifts of the PL peaks from wells no. 5 and no. 6 are further investigated in Fig. 5. To reduce influence from energy differences in the band gap of InGaAs caused by alloy fluctuations, the PL spectra are shown on an energy scale expressed as the energy shift from the PL peak of the InGaAs calibration layer. In general, the PL peaks shift toward higher energy for increasing etch time as indicated by the dotted lines. This figure also reveals that the high-energy shoulders of the peaks increase in intensity at the expense of the intensity of the low-energy shoulders and the main peak. We observe that the 10 ML peak increases relatively to the 11 ML peak and that the 6 ML peak increases relatively to the 7 ML peak. Also noted is a broadening of the PL peaks for increasing etch time. The same qualitative observations were made for the 149 W/428 V and the 248 W/543 V etches; however, the observed energy shifts were much smaller. The overall intensity of the PL spectra did not seem to be significantly affected by the RIE treatment, especially the quantum wells further away from the etched surface. For increasing etch time we observed a general narrowing of the PL peaks from the wider wells (no. 7 and no. 8) and the calibration layer, accompanied with an increase of the luminescence intensity. These observations seemed to be more pronounced for the high-energy etches. This is attributed to the passivation of nonradiative recombination centers by the low-energy H^+ ions.[15]

The origin of the shifts and the broadening of the PL peaks from the narrow quantum wells (no. 5 and no. 6) can be explained by intermixing of well and barrier materials at the interfaces, due to the low-energy ion bombardment during RIE. The slope of the well potential at the interface will decrease as the quantum-well layers are intermixed. Longer etch time results in lower effective slope. The confined state will experience an increased potential inside the well and a reduced potential outside the well. The shift in the confinement energy can be calculated using the results from first-order perturbation theory as the change of the potential weighted by the electron probability function. Since the

wave-function amplitude is larger inside the well, the confined states will experience an increase in the effective potential and the confinement energies therefore increase. The microroughness of the barriers is also expected to increase in the case of intermixing. This will lead to inhomogeneous broadening of the PL peaks as observed in the spectra. It is also expected that the in-plane exciton mobility will decrease. In this case the excitons are more likely to recombine at the positions where they are created rather than relaxing to the low-energy islands of the well before they recombine. With monolayer island formation at the interface this will result in an intensity shift from the low-energy shoulders to the high-energy shoulders of the wells as seen in the PL spectra. The smaller observed shifts for the high-energy etches are explained by the shorter etch times for corresponding higher bias voltages.

A quantitative estimate of the damage depth is difficult to give. We find that damage, as defined as a shift of the luminescence peaks, is confined to the upper seven quantum wells corresponding to a depth of 150 nm. A TRIM-90 Monte Carlo simulation showed that the range of the H^+ ions is less than 15 nm; however, due to channeling effects the ions are able to penetrate substantially deeper into the structure. We find no dependence of the damage depth of bias voltage for the present values.

In general, the effect of RIE treatment of these samples seems to indicate that intermixing at the quantum well interfaces is a non-negligible effect. This effect is proportional to the etch time and can be reduced by using high rf powers. Ion bombardment is apparently not generating defects that would reduce the luminescence intensity substantially for the quantum wells further away from the etched surface.

IV. SUMMARY

The influence of RIE processing of InP/InGaAs multiple-quantum-well structures has been investigated by low-temperature PL. A specially designed structure allowed the damage depth to be obtained from the PL spectra. The observed confinement energies for quantum wells thinner than 20 ML were smaller than expected from an envelope function calculation. This is explained by formations of InAsP islands at the interfaces of the wells as recently discussed by Böhrer and co-workers.[14] The presence of monolayer splittings of individual PL peaks enabled identification of their origin.

The samples etched by RIE in CH_4/H_2 showed only a small decrease in the luminescence intensity as compared to samples that had not been etched. The etch depths measured by the profilometer were in good agreement with the depths deduced from the PL measurements.

For increasing etch time, PL peaks also show shifts to higher energies. The shifts seemed to increase with etch time and were most pronounced for the samples etched with low bias voltage (rf power). The PL peaks originating from wells with monolayer fluctuations showed a general shift to higher energies as well as a shift in intensity from the low-energy shoulders to the high-energy shoulders. This can be explained by intermixing of well and barrier materials at the interfaces caused by the ion bombardment during the RIE

treatment. The effective narrowing of the wells causes larger confinement energies and explains the shifts of the PL peaks toward higher energies. The increased interface roughness causes a decrease of the in-plane exciton mobility and is responsible for the shifting of intensity from the low-energy shoulders to the high-energy shoulders of the monolayer splitted PL peaks. By increasing etch time it was observed that the PL peaks from the two widest wells and the calibration layer became more narrow and intense. This is caused by passivation of nonradiative recombination centers by the low-energy H^+ ions from the RIE process.

In conclusion, the RIE treatment did not severely degrade the sample quality. The low-energy bombardment by ions produced during RIE does not decrease the luminescence intensity substantially. However, prolonged etch times might result in intermixing of well and barrier materials causing energy shifts and broadening of the confined levels for thin quantum wells.

ACKNOWLEDGMENT

[1] J. N. Patillon, R. Gamonal, M. Iost, J. P. André, B. Soucail, C. Delalande, and M. Voos, J. Appl. Phys. **68**, 3789 (1990).

[2] J. Y. Marzin, A. Izrael, L. Birotheau, B. Sermage, N. Roy, R. Azoulay, D. Robein, J.-L. Benchimol, L. Henry, V. Thierry-Mieg, F. R. Ladan, and L. Taylor, Surf. Sci. **267**, 253 (1992).

[3] J. Werking, J. Schramm, C. Nguyen, E. L. Hu, and H. Kroemer, Appl. Phys. Lett. **58**, 2003 (1991).

[4] R. Germann, A. Forchel, M. Bresch, and H. P. Meier, J. Vac. Sci. Technol. B **7**, 1475 (1989).

[5] T. Kosugi, K. Gamo, S. Namba, and R. Aihara, J. Vac. Sci. Technol. B **9**, 2660 (1991).

[6] J. Hommel, M. Moser, M. Geiger, F. Scholz, and H. Schweizer, J. Vac. Sci. Technol. B **9**, 3526 (1991).

[7] D. L. Green, E. L. Hu, P. M. Petroff, V. Liberman, M. Nooney, and R. Martin, J. Vac. Sci. Technol. B **11**, 2249 (1993).

[8] C. Juang, J. K. Hsu, I. S. Yen, and H. S. Shiau, J. Appl. Phys. **72**, 684 (1992).

[9] G. Bastard, *Wave Mechanics Applied to Semiconductor Heterostructures* (Les éditions de Physique, Paris, 1988).

[10] *Semiconductors—Group IV Elements and III-V Compounds. Data in Science and Technology*, edited by O. Madelung (Springer, Berlin, 1991).

[11] D. V. Lang, M. B. Panish, F. Capasso, J. Allan, R. A. Hamm, A. M. Sergent, and W. T. Tsang, Appl. Phys. Lett. **50**, 736 (1987).

[12] Z. H. Lin, T. Y. Wang, G. B. Stringfellow, and P. C. Taylor, Appl. Phys. Lett. **52**, 1590 (1988).

[13] T. Y. Wang, E. H. Reihlen, H. R. Jen, and G. B. Stringfellow, J. Appl. Phys. **66**, 5376 (1989).

[14] J. Böhrer, A. Krost, and D. Bimberg, Appl. Phys. Lett. **60**, 2258 (1992).

[15] Y.-L. Chang, I.-H. Tan, C. Reaves, J. Mertz, E. Hu, S. DenBaars, A. Frova, V. Emiliani, and B. Bonanni, Appl. Phys. Lett. **64**, 5658 (1994).